Transactions of the Korean Nuclear Society Spring Meeting
Jeju, Korea, May 7-8, 2015

Assessment of MATRA-LMR-FB with the SHRT-17 Core Subassembly Data

Won-Pyo Chang, Jin Yoo, Seung Won Lee, Seung Hwan Seong, Sang June Ahn, Chi-Woong Choi, Kwi Lim Lee, Jae-Ho Jeong, Taekyeong Jeong, Kwi-Seok Ha*
Korea Atomic Energy Research Institute
P.O.Box 105, Yuseong, Daejeon, 305-600, Korea
**Corresponding author: wpchang@kaeri.re.kr*

1. Introduction

As a continuous study following the previous one [1], the present study completed the analysis of the SHRT-17(Shutdown Heat Removal Test 17) natural circulation test through input modeling improvements and successive comparison results. Since the MATRA-LMR-FB code is scheduled to be applied to a partial flow blockage analysis in a PGSFR (Prototype Generation IV Sodium-cooled Fast Reactor) subassembly, code verification is an essential part for the design review. Most of its verification efforts have been devoted to local sub-channel blockages, and thus the predictions were compared to those of other codes as well as experimental data [2, 3, 4, 5]. On the other hand, other aspects such as predictions on a radial temperature distribution in a subassembly and transient prediction capability were relatively overlooked. Verifications using pin bundles with a wire-wrap spacer had to be concentrated to 19-pin bundles, because available experimental data for such a bundle were relatively affluent in world-wide literatures. Therefore, more assessments with diverse pin numbers are necessary for MATRA-LMR-FB to be a more reliable code. Thus far, MATRA-LMR-FB has been applied to a 37-pin subassembly with wire-wrap spacers at most. In this regard, the present comparative study using data produced from the SHRT-17 which was carried out in a 61-pin test subassembly (XX09) placed in the EBR-II (Experimental Breeder Reactor II) core will be a meaningful demonstration for its extensive applicability.

The power operation of the EBR-II was begun by ANL (Argonne National Lab.) in 1964 and the SHRT program was carried out in EBR-II between 1984 and 1986 in order to provide not only test data for validation of the computer codes but also demonstration of a passive reactor shutdown and decay heat removal in response of the protected and unprotected transients [6].

2. Analysis

2.1 XX09 test subassembly in the EBR-II

The SHRT-17 was a loss of flow test and was performed on June 20, 1984 for demonstration of the effectiveness of natural circulation cooling characteristics. The transient was initiated by a trip of the primary and intermediate pumps. The reactor was also simultaneously scrammed to simulate a protected loss-of-flow accident. In addition, the primary system auxiliary coolant pump that normally had an emergency battery power supply was turned off. As the test continued, the reactor decay power decreased due to the fission product decay.

Figure 1 displays the cross-section of the XX09 subassembly along with the measurement positions. Elements #1 and #2 in the figure indicate no heat generation pins. Measured outlet subassembly temperatures for the steady state were compared with the MATRA-LMR-FB calculation results in the study, whereas the transient data could not be used because the inlet flow rate was out of the applicable range of MATRA-LMR-FB.

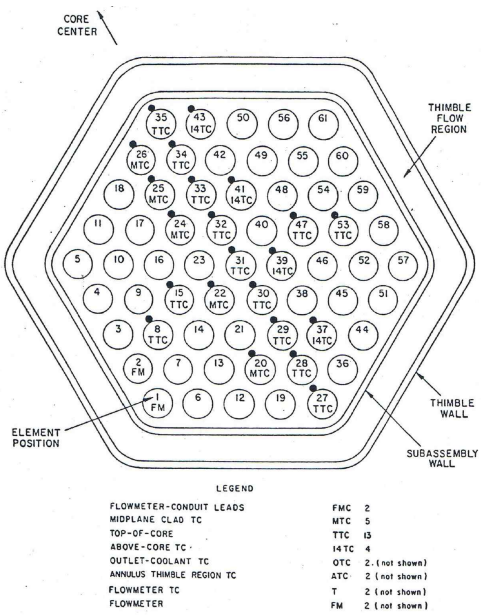

Fig.1. Pin arrangement and instrument loading in XX09

2.3 The MATRA-LMR-FB input

Table 1 summaries key MATRA-LMR-FB input parameters for the XX09 subassembly in the test. There are 13 radial positions for coolant temperature measurements as indicated with TTC near the core top (0.322 m), and 5 radial measurements (MTC) for the cladding surface temperature at the middle of the core (0.172 m) in Fig. 1. The axial heat flux distribution was provided in the active region with a calibrated power distribution from the test result. Since there were two pins (#1 and #2 in Fig. 1) with no heat generation, the total subassembly power was equally allocated to the

rest of 59 pins. Both the sub-channels and pin numbers were rearranged in accordance with the MATRA-LMR-FB numbering convention as shown in Fig. 2.

Table 1. Key input parameters for the SHRT-17 test

Parameters	Unit	Inputs
Number of pins		61
Number of unheated pins		2
Diameter of pin	inch	0.1736
Pin pitch	inch	0.2224
P/D		1.281
Total length of pin	inch	24.09
Active length of pin	inch	13.50
Wire-wrap pitch	inch	6.0
Diameter of spacer wire	inch	0.0488
Inner Flat-to-flat length	inch	1.827
Flow rates	kg/s	2.377
Power inputs	MW	0.393
Inlet temperature	^{o}F (^{o}C)	664.8 (351.6)

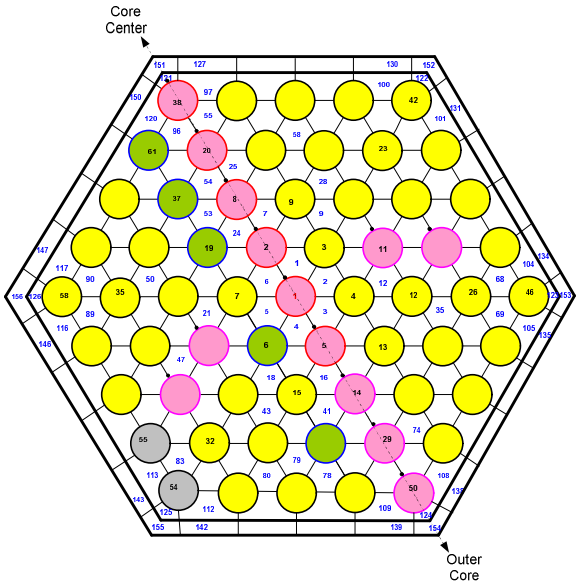

Figure 2. Cross-sectional configuration with sub-channel numbering in XX09 subassembly for MATRA-LMR-FB modeling

A preliminary study on node size was conducted to find a suitable size of the node, and MATRA-LMR-FB reached the steady state successfully within 4.0 s with all the node numbers. As a result, a node size in the neighborhood of 1-inch yielded stable solutions (Fig. 3) and the total active length of the sub-channels (0.343 m, 13.50 inches) was finally divided axially into 14 equally sized nodes.

2.3 Results and Discussions

Neither the thimble region flow nor the effective flow area was specified in the report [6]. As various measurement wires passed through the thimble region, the area could not be estimated exactly. Thus, a sensitivity study was carried out to find an effective thimble flow area which could provide a reasonable temperature distribution with 100%, 30%, 20%, and 15% of the total thimble flow area. Figure 4 compares the coolant temperatures depending on the effective thimble flow areas. Although the effective area might be reduced, the calculated temperatures never approached to the data.

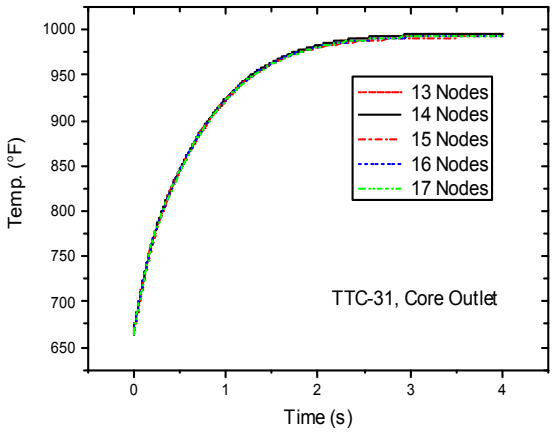

Fig. 3 Node dependency on outlet subassembly for the steady state (TTC-31)

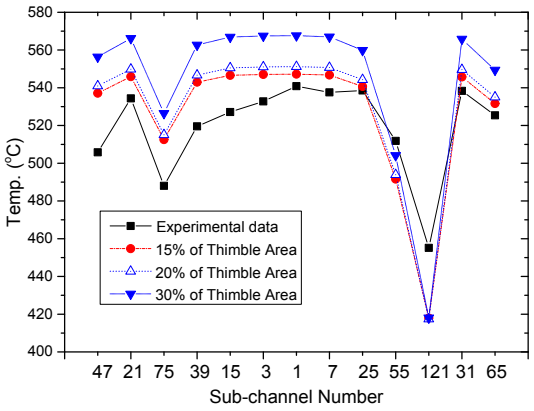

Fig. 4. Comparison of sub-channel temperature (TTC) distribution

According to a discussion during a CRP (Cooperated Research Project) meeting [7], it was informed that roughly around 10% of the total inlet flow entered the thimble region. Figure 5 compares temperature distributions with applying 10% flow allocation to the thimble region as a boundary inlet flow condition. As one might expect, the distribution was converged regardless of the flow areas. However, temperatures in sub-channels #47 and #75 were over-predicted, while temperature in sub-channel #121 was especially under-predicted. The over-prediction in sub-channel #47 was probably caused by the effect of dummy pin number #55

in Fig. 2. As a measurement, TTC-8, was attached at the boundary between sub-channels #47 and #86, it must be influenced by a sub-channel surrounding dummy pin #55 through sub-channel #86. Figure 6 compares axial temperature profiles for the sub-channels around pin #33 including a sub-channel surrounding dummy pin #55. A lower temperature was anticipated for sub-channel #86 because it was a sub-channel next to sub-channel #85. However, the temperature in sub-channel #86 was higher than expected. Such temperature difference between sub-channels #85 and #86 indicated that there was almost no cross-flow between them. If there had been an active cross-flow between them, temperature difference would not be as large as that shown in Fig. 6. On the other hand, active mass and energy exchange could be imagined between sub-channel #47 and adjacent sub-channels, because the temperature in sub-channel #47 was comparable to those sub-channels in magnitude. The result supported a possible speculation that MATRA-LMR-FB was not able to represent such cross flow pattern as well as the effect of a colder sub-channel #85 realistically.

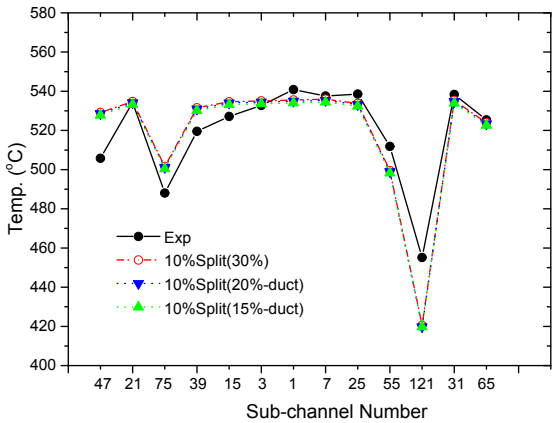

Fig. 5. Comparison of sub-channel temperature (TTC) distribution applying a boundary condition of 10% flow into the thimble

The problem was still left with the over- and under-predictions in sub-channels #75 and #121, respectively. It was considered that coolant mixing associated with cross-flow between neighboring sub-channels in those regions might affect the distribution, and such a cross-flow pattern which was inferred from the test data seemed not to be predicted realistically by the code. A considerably lower temperature was predicted in sub-channel #121, owing to relatively small amount of heat transfer from the fuel pins into a corner sub-channel such as sub-channel #121 than other sub-channels such as #97 or #55 without active coolant mixing around. The over-prediction of temperature in sub-channel #75 might attribute to the prediction of excessive coolant mixing between #108 and #75, even though it could not be observed directly in the test.

As an alternative modeling to reduce the discrepancy,

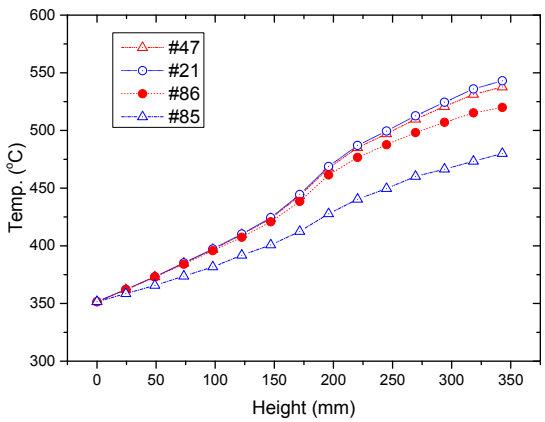

Fig. 6. Sub-channel temperature (TTC) profiles near dummy pin #55

corner sub-channels such as #121 were consolidated into each adjacent edge sub-channels as illustrated in Fig. 7. As a result, the temperatures in sub-channels #75 and #121 were predicted favorably closer to the

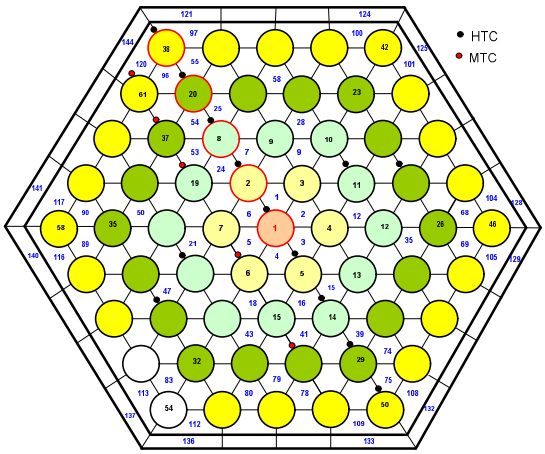

Fig. 7. Cross-sectional configuration of an alternative sub-channel modeling with consolidated corner sub-channels

corresponding test data in Fig. 8. Nevertheless, the code failed to predict a radially ascending trend toward the core center observed in the test. The prediction was almost flat distribution in the radial sub-channels along the A-A' line in Fig. 2, i.e., the channels from #75 through #121 in Fig. 8. Various calculations were conducted to elucidate the mismatch. A conclusion was reached that there might be a distribution in the pin power within the subassembly so that roughly half of the pins positioned near the core center region as illustrated Fig. 9 were modeled at a higher pin power than the other pins arrayed in a side of the outer core by 6%. The figure corresponded to the amount of the heat generation from the two dummy pins if they generated an average pin power as if all the 61 fuel pins were contributed to the subassembly coolant heat-up. The rest of pins kept the average pin power. As shown in Fig. 8, the calculation result for the temperature distribution

revealed a similar trend as that of the test data. From the comparison, it could be drawn out that there existed a pin power distribution inside the subassembly.

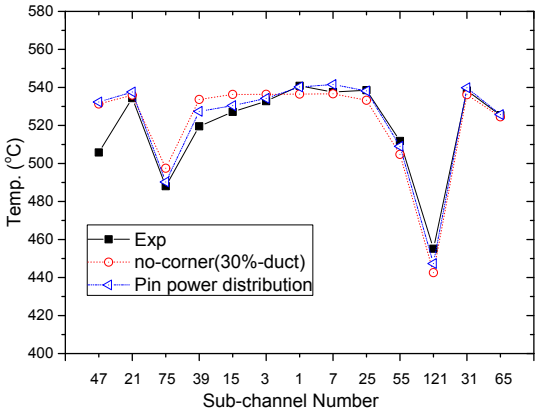

Fig. 8. Comparison of temperature distribution with consolidated corner sub-channels and pin power distribution

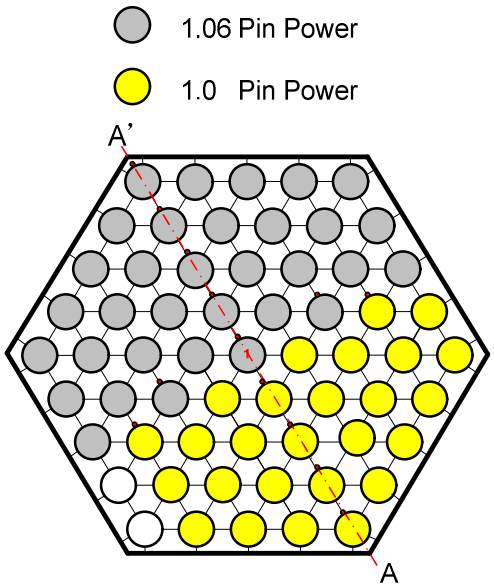

Fig. 9. Modeling of pin power distribution

Figure 10 compares 5 data points for the cladding temperatures at the axial mid-plane, which are indicated with 'MTC' in Fig. 1. It also showed some discrepancy for a pin positioned near the outer core (#30). It was considered that the radial flow distribution associated with cross flow might be a main factor affecting the result.

3. Conclusion

The EBR-II SHRT-17 test data were used to demonstrate the prediction capability of MATRA-LMR-FB on a radial distribution of the subassembly outlet temperatures during the steady state. As a result, the code could predict reasonably the trend of the radial distribution as well as the magnitudes for the radial distribution of the subassembly outlet temperatures through the sub-channel input modeling adjustment and an assumption of a pin power distribution inside the subassembly. There still existed a discrepancy in the prediction of the cross flow pattern near the dummy pins. It is not possible to catch the cause exactly at the present time, because there were no corresponding test data to be compared. Therefore, only an inference was proposed in the analysis.

However, limitation of the code applicability was also found in the transient calculation. Before the present analysis, the lowest flow rate examined for MATRA-LMR-FB was 1.9 kg/s for the 19-pin tube bundles. The code failed to obtain a converged solution with a lower flow than roughly 0.071 kg/s (3% of the normal inlet flow), or a transient faster than about 0.56×10^{-3} °C/s. Finally, the MATRA-LMR-FB code is not favorable in a simulation of transients with a low flow rate.

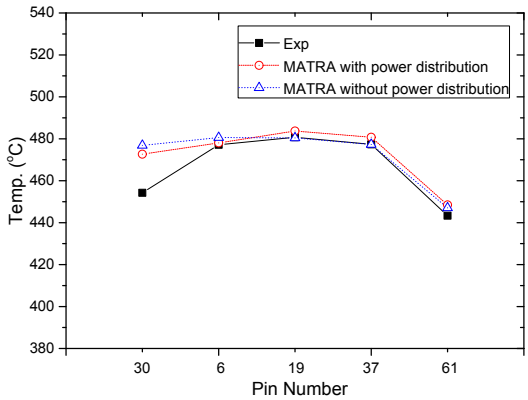

Fig. 10. Comparison of cladding temperature (MTC) distribution

REFERENCES

[1] Won-Pyo Chang, Jin Yoo, Chi-Woong Choi, Kwi-Seok Ha., 2014. A study on a MATRA-LMR-FB prediction capability with an EBR-II natural circulation test. Transactions of the Korean Nuclear Society Autumn Meeting, Pyeongchang, Korea, October 30-31, 2014.

[2] Ha, K. S., Jeong, H. Y., Chang, W. P., Kwon, Y. M., Cho, C. H., and Lee, Y. B., 2009. Development of the MATRA-LMR-FB for Flow Blockage Analysis in a LMR," Nucl. Eng. Tech. 41, 6, 797-806.

[3] Jeong, H. Y., Ha, K. S., Chang , W. P., Kwon, Y. M., and Lee, Y. B., 2005. Modeling of Flow Blockage in a Liquid Metal–Cooled Reactor Subassembly With a Subchannel Analysis Code. Nuclear Technology 149, 71-87.

[4] H.-Y. Jeong, K.-S. Ha, Y.-M. Kwon, Y.-B. Lee, D. Hahn., 2009, Analysis of three different types of blockage in a sodium flow path with the MATRA-LMR-FB code. Annals of Nuclear Energy 36 (2009) 583-589.

[5] Chang, W.P., Ha, K.S., S.D. Suk, Cheong, H.Y., 2011. A Comparative study of the MATRA-LMR-FB Calculation with the SABRE result for the flow blockage accident in the sodium cooled fast reactor. Nucl. Eng. Des. 241, 5225-5237.
[6] T. Sumner and T.Y. C. Wei, 2012. "Benchmark Specifications and Data Requirements for EBR-II Shutdown Heat Removal Tests SHRT-17 and SHRT-45R," ANL-ARC-226 (Rev 1), (May 31, 2012).
[7] SUMMARY REPORT on First (KICK-OFF) Research Coordination Meeting (RCM) of the IAEA Coordinated Research Project (CRP) on "Benchmark Analysis of an EBR-II Shutdown Heat Removal Test," 18-19 June 2012, Argonne National Laboratory, USA.